The role of catalyst in controlling N_2 reduction selectivity: a unified view of nitrogenase and solid electrodes

Alexander Bagger,*,† Hao Wan,† Ifan IE Stephens,‡ and Jan Rossmeisl†

†*Department of Chemistry, University of Copenhagen, Universitetsparken 5, Copenhagen, Denmark*

‡*Royal School of Mines, Imperial College London, South Kensington Campus, London, UK*

E-mail: *alexander@chem.ku.dk

Abstract: The Haber-Bosch process conventionally reduce N_2 to ammonia at 200 bar and 500 degree Celsius. At ambient conditions, i.e. room temperature and ambient pressures, the N_2 can be converted into ammonia by the nitrogenase molecule and lithium-containing solid electrodes in non-aqueous media. In this work, we explore the catalyst space for N_2 reduction reaction at ambient conditions. We describe N_2 reduction on the basis of the $*N_2$ binding energy versus the *H binding energy; we find that under standard conditions, no catalyst can bind and reduce $*N_2$ without producing H_2. We show why a selective catalyst for N_2 reduction will also likely be selective for CO_2 reduction, but N_2 reduction is intrinsically more challenging than CO_2 reduction. Only by modulating the reaction pathway, like nitrogenase, or tuning chemical potentials, like the Haber-Bosch and the Li-mediated process, can N_2 be reduced.

Keywords:Classification, N_2 reduction, CO_2 reduction, CO reduction, Electrochemistry, Electrocatalysais, Density functional Theory

The reduction of N_2 to NH_3 is a critical process for the growth of plants in nature and for the chemical industry. Ammonia is the key feedstock for the nitrate fertilizers; moreover, there is growing interest in the use of ammonia as a sustainable carbon-free fuel.[1] The nitrogen molecule is highly abundant in the atmosphere; however, the nitrogen molecule is extremely difficult to activate. Today, all N_2 is fixated primarily via two routes: i) the industrial Haber-Bosch process, which takes place at high-temperatures and pressures[2] and ii) the biological nitrogenase enzyme, which takes places at ambient temperatures and pressures.[3] Ammonia synthesis via the Haber Bosch process is an efficient process, but it consumes H_2, which is typically delivered from Steam Methane Reforming (SMR). In total ammonia synthesis from Haber Bosch with SMR consumes more energy and produces more CO_2 than other chemicals. The limitations of Haber Bosch has driven researchers towards the discovery of a more sustainable but scalable alternative.[4–7]

The electrochemical reduction of N_2 at ambient temperatures and pressures on solid electrodes is particularly attractive. Metal electrodes in aqueous solution produce such low yields of ammonia that is impossible to distinguish the desired product from background contamination.[8] Thus far, only studies on Li containing electrodes in organic electrolytes (Ethanol and THF-containing) provide unequivocal proof that N_2 reduction is possible on a solid electrode.[9–12]

Density functional theory studies of N_2 electroreduction have focused on transition metals,[13–15] lithium based surfaces,[12] metal doped carbons[16] or nitrogenase,[17] all in isolation, but—to the best of our knowledge—not in comparison to each other. Such studies have emphasized the role of tailored electron and proton transport to the active site,[18] and scaling relations between the binding energies of *H (where * denotes an adsorbed species) and more protonated intermediates, such as *N2H, leading to volcano plots to describe trends in activity. Strategies are needed to break these linear scaling relationships,[19] one example could be metal-ionic liquid interfaces for electrochemical Nitrogen reduction,[20] however, we note doubts have been cast on the veracity of the experimental proof that these interfaces are able to reduce N_2 to NH_3, both by the original authors (see Supplementary Information of ref[8]) and Kibsgaard et al.[21]

N_2 reduction is somewhat analogous to CO_2 reduction: both reactions require a high overpotential, and both compete directly with H_2 evolution.[22] Curiously, nature suggests that there could be a fundamental link between CO_2 and N_2 reduction: nitrogenase is the only enzyme that can reduce CO_2 via CO into energy rich multielectron products: ethylene, ethane, propylene, propane, a-butylene, n-butane, and methane.[23–25]

Our working hypothesis is that the binding energies of relevant intermediates will determine trends in catalytic properties of each catalyst investigated, without knowing the exact reaction pathway. This is under the assumptions that (a) the catalysts are affected similarly by the electrochemical environment, (b) that the trends in low coverage regime capture the most important features of the catalyst performance , (c) while we only investigate a limited number of active sites for each material, that the trends we observe will also roughly correlate to those on other facets, including defects and (d) we acknowledged that selectivity can be matter of very small energy differences which can be challenging for DFT methods, however the eV scale analyssis made here give robustness in our conclusions.

In the current study, we will apply the classification scheme we previously used for CO_2 reduction reaction (CO_2RR) to understand trends in N_2 reduction reaction (N_2RR) selectivity. In particular, we focus on the key challenge in N_2 reduction: to reduce N_2 without making H_2 (Hydrogen Evolution Reaction, HER).[26] We show that our pared down and unified approach can describe a wide range of catalysts, including (i) nitrogenase, shown in Figure 1a (ii) metal and nitrogen-doped carbon MN4-C, where M is a transition metal, shown in Figure 1b (iii) pure transition metals, shown in Figure 1c and (iv) Li-containing surfaces, shown in Figure 1d.

We consider the three reactions of interest on the catalyst

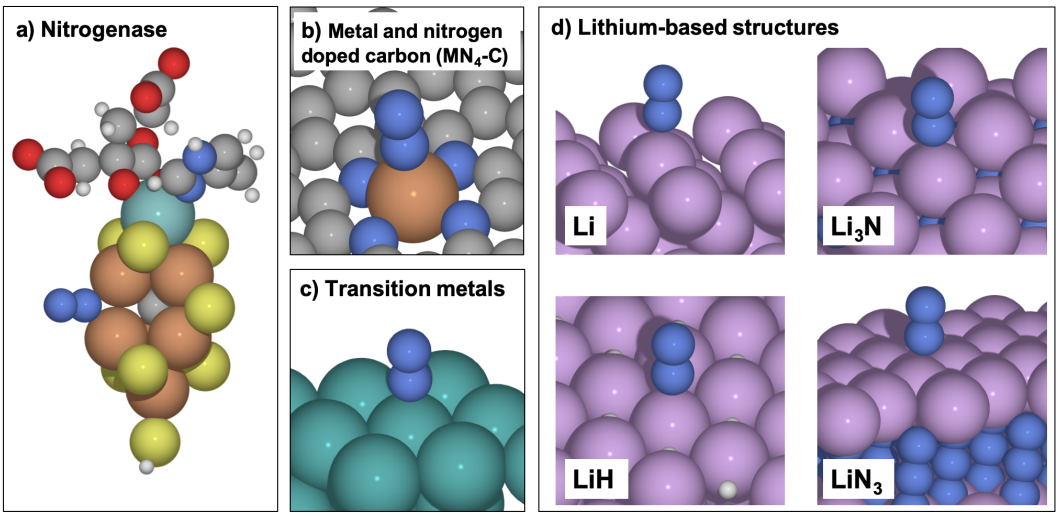

Figure 1. Atomistic structure illustration of a) the nitrogenase cluster with N_2 placed at the sulphur-belt position, b) metal and nitrogen-doped carbon (MN_4-C) structure, c) the metallic face centred cubic (111) facet and d) Li structures used for simulation with the ontop vertical adsorption of both CO and N_2, whereas Li is so activate that in some cases both CO and N_2 adsorps stronger in a horizontal position (C atoms are gray, N blue, H light gray, S yellow, O red, Li purple, Fe orange, unspecified transition metals are turquouise).

according to the following generalized form:

$$\mathrm{CO_2RR:}\ \left(\mathrm{H^+ + e^-}\right) + \mathrm{CO_2} \rightarrow {}^*\mathrm{CO} \rightarrow \mathrm{C}_x\mathrm{H}_y\mathrm{O}_z \quad (1)$$

$$\mathrm{N_2RR:}\ \left(\mathrm{H^+ + e^-}\right) + \mathrm{N_2} \rightarrow {}^*\mathrm{N_2} \rightarrow \mathrm{N}_x\mathrm{H}_y \quad (2)$$

$$\mathrm{HER:}\ \left(\mathrm{H^+ + e^-}\right) \rightarrow {}^*\mathrm{H} \rightarrow \tfrac{1}{2}\mathrm{H_2} \quad (3)$$

Here we consider binding *CO, $^*N_2$ and *H as a prerequisite for the reduction reaction to proceed and the direct comparison of the binding energies allow us to create reduction reaction criteria. Figure 2a shows our classification scheme to describe trends in selectivity for CO_2 electroreduction on metals[27] and nitrogen-doped carbon.[28] The prerequisite for reducing CO_2 to hydrocarbons and oxygenates is that the catalyst must enable CO reduction, otherwise the reaction stops with CO.

> **CORR criterion:** *Selective CO reduction requires a catalyst that adsorbs *CO and does not adsorb *H.*

This criterion is rather intuitive; if the surface is covered with hydrogen, there is a high probability for H_2 evolution than CO_2 reduction, as is the case for Pt or Fe; if CO desorbs from the surface, its further reduction to hydrocarbons and oxygenates is unlikely, as is the case for Ag or In. All pure metals and MN_4-C structures follow this criterion.

Herein we establish an analogous criterion for N_2 reduction:

> **N_2RR criterion:** *Selective N_2 reduction requires a catalyst that adsorbs $^*N_2$ but does not adsorb $^*H$.*

For the electrochemical reduction of N_2, we consider the formation of $^*N_2$ to be more critical in controlling selectivity than other potential intermediates, such as (i) the first protonated intermediate, $^*N_2H$,[29] or (ii) *N, from dissociating N_2 at high temperatures, (e.g. in the Haber-Bosch process).[2] Analogously, for CO_2 reduction, the formation of *CO is more critical in controlling selectivity than the formation of (i) more protonated intermediates such as *CHO and *COH states or (ii) *C and *O, formed by dissociating CO_2 or CO at high temperatures (e.g. during Fischer Tropsch[30]). One should note the difference in the two criteria when comparing CO_2 and N_2 reduction. The criteria for CO_2 is related to CO reduction to high value products, although it does allow to distinguish the H_2, CO, formic acid and high value products.[31] While for N_2 reduction, the reduction does not allow other products ("easy" products), and there is currently less experimental evidence to support the criteria as N_2 reduction in aqueous electrolytes is highly challenging and produces primarily competitive H_2.

Figure 2 shows the binding energies of $^*N_2$, *CO and *H for the Nitrogenase (green triangles), metal-nitrogen-carbon/MN_4-C (black dots), Li-mediated structures (magenta square) and metal catalysts (blue crosses).

Figure 2a shows the base plot for identifying product distributions from CO_2 reduction reaction catalyst by using the *CO and *H binding energies as descriptors. The vertical line depicts ΔG_{H^*}=0 for $\frac{1}{2}H_2 \leftrightarrow$ H* or the same as $H^+ + e^- \leftrightarrow$ *H at 0 V_{RHE}. This allows to distinguish catalysts for which *H adsorption is exogenous at 0 V versus a reversible hydrogen electrode. In electrochemical terms, this means that they exhibit underpotential deposition (UPD) of *H. The catalyst that have $^*H_{UPD}$ primarily produce H_2 under CO_2 reduction conditions. The horizontal line divides catalysts that can bind *CO under standard conditions versus those that cannot. Unique amongst metals, Cu can bind *CO without *H under standard conditions, hence giving rise to a series of high energy multi-electron products including CH_4, C_2H_4 and C_2H_5OH.[33,34] Notably, FeN_4-C, MnN_4-C and CoN_4-C are in the same quadrant as Cu; those materials also yield small amounts of more reduced products, such as CH_4, from CO_2 reduction.[35,36]

On Figure 2a, we have plotted the pristine, (unactivated) nitrogenase as the filled triangles; The iron molybdenum (FeMo), iron vanadium (FeV) and iron (FeFe) nitrogenase binds *H similarly around the vertical line. FeMo and FeV, does not bind *CO. FeFe binds *CO slightly, bordering on the fourth quadrant, i.e. it should, in principle, yield energy-rich products during CO or CO_2 reduction. However, experiments show that *CO binds by replacing a belt-sulphur

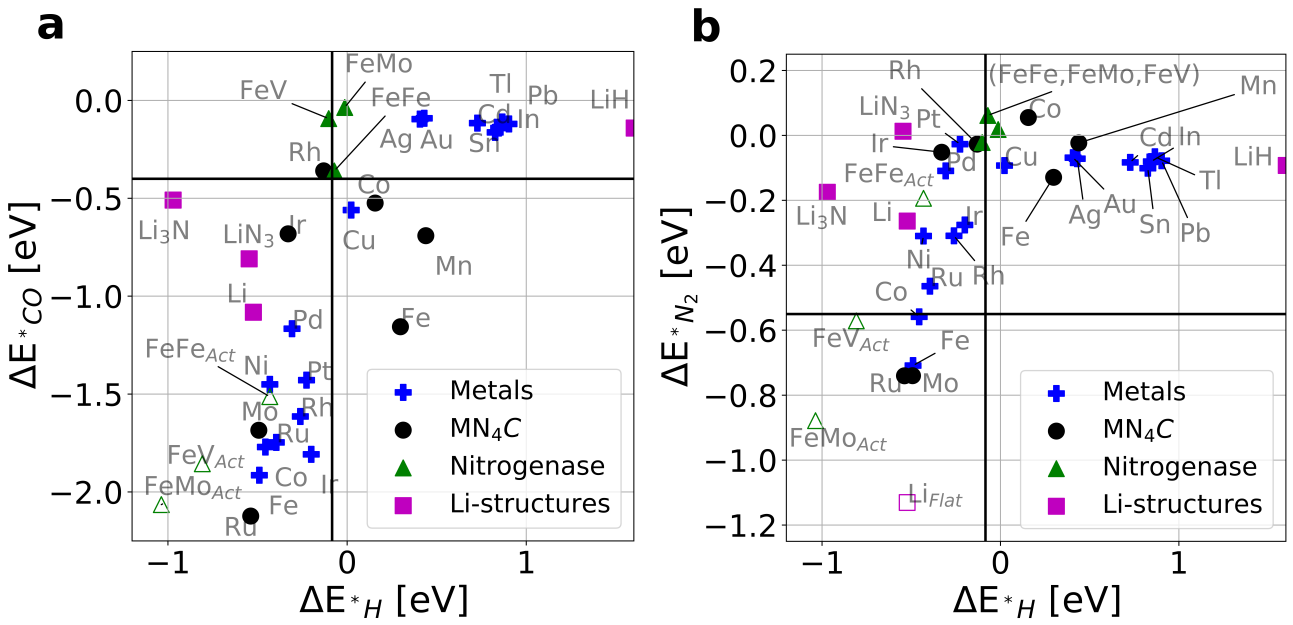

Figure 2. a) Classification scheme for CO_2 reduction, with the *CO binding energy ΔE_{*CO} plotted as a function of *H binding energy, ΔE_{*H} (Metal and MN_4-C data from[27,28]). b) show the $*N_2$ vs *H binding energies for N_2 reduction reaction in aqueous solution at ambient conditions. The vertical line depicts $\Delta G_{H^*}=0$ for $\frac{1}{2}H_2 \leftrightarrow H^*$, while the horizontal lines show CO(g) vs. *CO and N_2(g) vs $*N_2$, respectively, under standard conditions. Nitrogenase binding energies for Iron Molybdenum (FeMo), Iron Vanadium (FeV) and Iron (FeFe) is shown as initial state (filled green triangle marker) and as an activated state (empty green triangle marker). The activated state of the cluster is with the sulphur removed from the active site by SH_2.[32] Li_{flat} is added as there is no barrier from a vertical $*N_2$ to a flat lying $*N_2$ at Li(empty magenta square marker). Note that LiH is a semiconductor and that *H binding for LiH is from removing *H from a stoichiometric surface, rather than adding *H, as this requires 1 eV more.

atom;[37] we have plotted the binding energies of these activated nitrogenase cofactors as the hollow triangles (with a sulphur removed as SH_2); according to Figure 2a, these activated structures bind both *CO and *H strongly. In other words, based on this plot, which takes into account the most thermodynamically favoured binding site, we would expect the activated nitrogenase to favour H_2 over more reduced CO reduction products.

Interestingly, Li_3N, LiN_3 and Li also occupy the lower left quadrant in Figure 2a, meaning they should favour H_2 evolution. Substoichometric LiH occupies the upper right quadrant, meaning that it is quite inactive. However, LiH in stoichiometric form is a semiconductor in our simulation, which would mean it would be unable to deliver electrons and function as an electrocatalyst; hence we do not consider it likely to be the experimentally active phase. Removing *H allows LiH to be conducting; however, since the Fermi Level changes upon adsorption, the binding energy that we calculate may be an artefact, as we recently found to be the case for O_2 evolution.[38]

Figure 2b is a similar base plot shown for N_2RR by plotting the $*N_2$ and *H energy binding energies as descriptors. The vertical line again depicts $\Delta G_{H^*}=0$ for $\frac{1}{2}H_2 \leftrightarrow H^*$ and the horizontal line shows the thermodynamic N_2(g) versus $*N_2$ adsorbed. It should be noted that the y-scale of Figure 2a and 2b are not equal. The thermodynamics of *CO and $*N_2$ adsorbed is similar, however, the binding energies of $*N_2$ are much weaker than *CO, by around 1 eV. Those catalysts that are able to bind N_2 at ambient condition include Fe metal, Co metal, MoN_4-C and RuN_4-C. However, those catalysts also bind *H too strongly, meaning that they should, in principle, favour H_2 evolution over N_2 reduction.

Figure 2b suggest that even the strongest binding transition metals, such as Fe and Ru (which are also the industrial Haber Bosch catalysts[2]) exhibit weak, close to thermoneutral binding to N_2 under ambient conditions. However, Figure 2b shows that MoN_4-C and RuN_4-C bind $*N_2$ stronger than transition metals under standard conditions, suggesting they may show greater promise for N_2 electroreduction; nonetheless, the delivery of protons to $*N_2$ could be a challenge on these isolated single site catalysts, as we recently showed to be the case for *CO protonation on FeN4-C during CO_2 reduction.[39]

Curiously, the Li-mediated structures does not have $*N_2$ adsorption in the vertical end-on position typical of low index planer metal surfaces. However, undergoing $*N_2$ dissociation, we observe that for Li there is no barrier to lie down flat. In this position the $*N_2$ adsorption is favoured and this point is marked as Li_{flat}. The Li system is instead challenged by HER, as *H binds strongly and hence the structures are in the HER region. This goes hand in hand with the observation that in aqueous electrolytes the Li-mediated system produces primarily HER.[10] If the chemical potential of protons is significantly lowered, through the use of non-aqueous solvent, the vertical line moves to the left in Figure 2a,b. In this case, the *H binding towards HER will gets suppressed and NH_3 formation is observed; presumably the ethanol acts as a sacrificial proton donor.

The modelled nitrogenase cofactor, in Figure 2b, with iron (FeFe), iron-molybdenum (FeMo) & iron-vanadium (FeV) is in the upper right square, with close to thermoneutral *H binding line, consistent with the superior properties of nitrogenase as a catalyst for H_2 evolution.[42] However, it also illustrates that the cofactor in the pristine state does not bind $*N_2$. Conversely, activated nitrogenase cofactors the Molybdenum ($FeMo_{Act}$) and Vanadium (FeV_{Act}) bind $*N_2$,

but also bind *H strongly. However, the fact that nitrogenase can reduce N_2 and CO_2 without producing copious amounts of H_2 suggests nature has found a trick to circumvent the scaling relation shown in Figures 2a and 2b. This can be due to i) putatively by providing sequential access to protons and electrons from the environment around nitrogenase and ii) the reversible adsorption and desorption of the SH_2 group during each catalytic cycle.[18,43] We consider that the SH_2 desorption and N_2 adsorption must be a concerted reaction, and the SH_2 desorption can not happen concertedly with a proton. A perspective of the nitrogenase trick "adsorption and desorption of the SH_2 cycle" is to used the nitrogenase as an electrocatalyst, however this has shown stability issues when tested.[44]

Importantly, Figure 2 shows that in terms of binding energies of *CO, *H and *N_2, there are negligible differences between metal doped carbon, transition metals, nitrogenase and lithium structures: they all fall on the same line.

The increased pressure provided by Haber-Bosch conditions move the thermodynamic N_2 line upwards, allowing metal Ru and Fe, to bind N_2. Further, when the N_2 reaction is not limited by *N_2 adsorption (due to high pressure), the high temperatures of the Haber Bosch allows the N_2 molecule to be in direct equilibrium with *N at the surface. As the Li_{flat} structure is not limited by *N_2 adsorption, the coverage of *N_2 could be higher for the lithium-based system before it turns into a bulk nitride, which may challenge the low-coverage assumption made for the simulations and perturb the binding energies presented for Li. However, for the goal of comparing the lithium-mediated system to other materials in this work, we find the low coverage simulations sufficient. When comparing materials for N_2 reduction lead us to investigate if Li mimics Haber-Bosch Ru and Fe - allowing the Li phase to be directly in equilibrium with *N at the surface even at low temperature.

Figure 3, show the N_2 dissociation barrier at Fe, Ru and Li. The barrier for dissociating N_2 on Fe and Ru is 0.4 eV[40]).

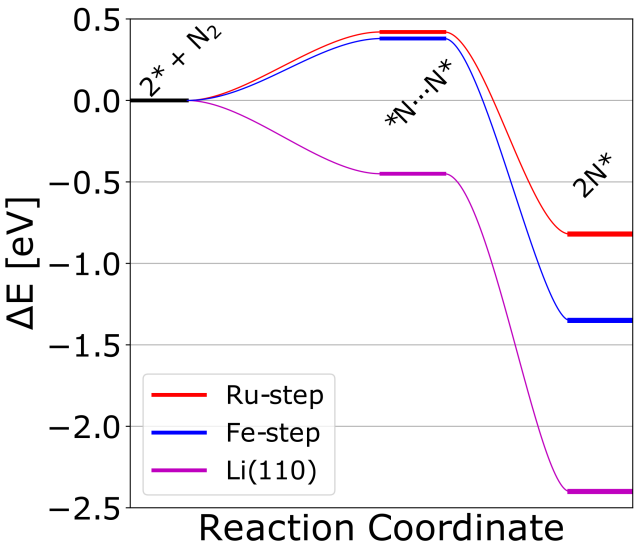

Figure 3. N_2 dissociation barrier on metallic Fe-step, Ru-step and body centered cubic (110) of Li from reference.[40,41] Fe-step and Ru-step have similar barrier (0.4 eV), but slightly split here for visual purpose a large barrier, while Li does not have a barrier. This allows Li to bind and dissociate N_2 at ambient pressure and temperature.

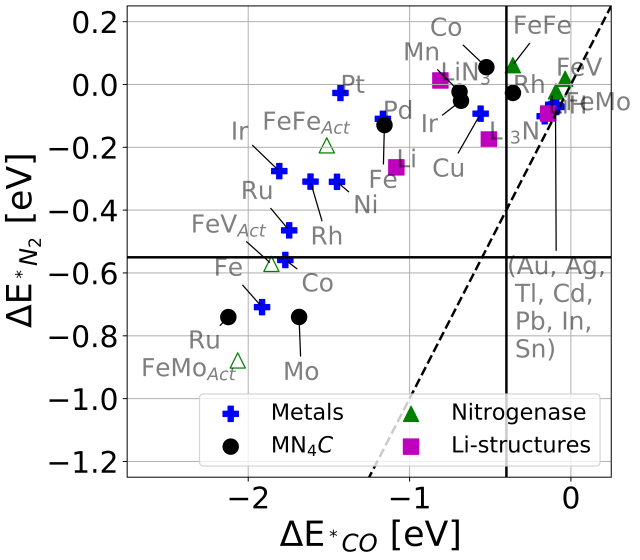

Figure 4. Binding energies of *N_2 versus *CO. All points is above the dashed line given as *N_2 = *CO shows that binding *CO is easier at ambient conditions, hence CORR should be easier than N_2RR. Note that a series of metal catalyst is on the diagonal line, due to the fact that they do not bind CO or N_2.

Comparing with Li, the barrier to dissociate is negligible.[41] This shows that active Li can dissociate N_2 to *N at low temperature. However, we do not envisage that low barriers for N_2 dissociation are a prerequisite for electrochemical N_2 reduction: experiments on nitrogenase shows that the scission of the nitrogen-nitrogen bond occurs after substantial hydrogenation of the N_2 in its adsorbed state, i.e. via an associative pathway.[45] As such, we conjecture that other solid electrodes, apart from those based on Li, may reduce N_2 as long as (a) like nitrogenase, they are able to bind N_2 in the first place, even if they adsorb in the end-on form and (b) that the barriers for the downstream hydrogenation of N-containing intermediates can be easily surmounted and (c) the chemical potential of protons, electrons and N_2 are suitably controlled.

Finally, a comparison between N_2RR and CO_2RR is carried out at ambient conditions. Figure 4 shows the *N_2 binding energy versus the *CO binding energy. The vertical and horizon lines note the thermodynamics of binding at ambient conditions, while the dashed diagonal line compared *N_2 = *CO. The binding energies for the catalyst systems investigated here lie above the diagonal line, except those in the top right hand quadrant, that bind neither CO nor N_2, which lie right on the diagonal in the upper right corner. The observation that no materials lie below the diagonal line, shows that binding *CO is much easier than binding *N_2. Hence we establish that N_2 is intrinsically more challenging to catalyse than CO_2 reduction; however, a good catalyst for N_2 reduction would likely be an excellent catalyst for CO_2 reduction.

Our *N_2 vs *H view on N_2 reduction under ambient conditions, encompassing a broad range of catalysts, shows that the catalysis of N_2 reduction under ambient pressure and temperature and aqueous electrolyte is challenging, even on nitrogenase. Driving the catalysis efficiently requires going beyond judicious choice of the catalyst material by either:

(i) Having the right chemical potentials of N_2 and temperature (Haber-Bosch),

(ii) Having the right chemical potentials of protons (lithium mediated system),

(iii) Having a concerted N_2 adsorption with a desorption reaction, e.g. SH_2 (nitrogenase),

(iv) Or by delivering the protons sequentially (nitrogenase).

We propose a possible route to sustain efficient N_2 reduction is - by considering electrocatalysis in 3D - to control the properties of the electrolyte delivering protons at the active site, as the hangman motif[46] or diporphyrin molecules.[47]

Structures with total energies and plotting method is available on the webpage: `https://nano.ku.dk/english/research/theoretical-electrocatalysis/katladb/n2rr/`.

Supporting Information contains a description of the computational details and computational structures. This information is available free of charge on the ACS Publications website **Acknowledgement** AB, HW and JR acknowledges the Danish National Research Foundation centers of excellence, The Center for High Entropy Alloys Catalysis (Project DNRF149). IELS acknowledges funding from the European Research Council (ERC) under the European Union's Horizon 2020 research and innovation programme (grant agreement No. 866402)

References

(1) *Ammonia: zero-carbon fertiliser, fuel and energy store*; The Royal Society, 2020; An optional note.

(2) Ertl, G. Primary steps in catalytic synthesis of ammonia. *Journal of Vacuum Science & Technology A* **1983**, *1*, 1247–1253.

(3) Hinnemann, B.; Nørskov, J. K. Chemical Activity of the Nitrogenase FeMo Cofactor with a Central Nitrogen Ligand: Density Functional Study. *Journal of the American Chemical Society* **2004**, *126*, 3920–3927.

(4) Chen, J. G.; Crooks, R. M.; Seefeldt, L. C.; Bren, K. L.; Bullock, R. M.; Darensbourg, M. Y.; Holland, P. L.; Hoffman, B.; Janik, M. J.; Jones, A. K.; Kanatzidis, M. G.; King, P.; Lancaster, K. M.; Lymar, S. V.; Pfromm, P.; Schneider, W. F.; Schrock, R. R. Beyond fossil fuel-driven nitrogen transformations. *Science (New York, N.Y.)* **2018**, *360*.

(5) Comer, B. M.; Fuentes, P.; Dimkpa, C. O.; Liu, Y.-H.; Fernandez, C. A.; Arora, P.; Realff, M.; Singh, U.; Hatzell, M. C.; Medford, A. J. Prospects and Challenges for Solar Fertilizers. *Joule* **2019**, *3*, 1578 – 1605.

(6) Lazouski, N.; Chung, M.; Williams, K.; Gala, M. L.; Manthiram, K. Non-aqueous gas diffusion electrodes for rapid ammonia synthesis from nitrogen and water-splitting-derived hydrogen. *Nature Catalysis* **2020**, *3*, 2520–1158.

(7) Cui, X.; Tang, C.; Zhang, Q. A Review of Electrocatalytic Reduction of Dinitrogen to Ammonia under Ambient Conditions. *Advanced Energy Materials* **2018**, *8*, 1800369.

(8) Choi, J.; Suryanto, B. H. R.; Wang, D.; Du, H.-L.; Hodgetts, R. Y.; Ferrero Vallana, F. M.; MacFarlane, D. R.; Simonov, A. N. Identification and elimination of false positives in electrochemical nitrogen reduction studies. *Nature Communications* **2020**, *11*, 5546.

(9) Andersen, S. Z.; Čolić, V.; Yang, S.; Schwalbe, J. A.; Nielander, A. C.; McEnaney, J. M.; Enemark-Rasmussen, K.; Baker, J. G.; Singh, A. R.; Rohr, B. A.; Statt, M. J.; Blair, S. J.; Mezzavilla, S.; Kibsgaard, J.; Vesborg, P. C. K.; Cargnello, M.; Bent, S. F.; Jaramillo, T. F.; Stephens, I. E. L.; Nørskov, J. K.; Chorkendorff, I. A rigorous electrochemical ammonia synthesis protocol with quantitative isotope measurements. *Nature* **2019**, *570*, 504–508.

(10) Tsuneto, A.; Kudo, A.; Sakata, T. Lithium-mediated electrochemical reduction of high pressure N2 to NH3. *Journal of Electroanalytical Chemistry* **1994**, *367*, 183 – 188.

(11) Lazouski, N.; Schiffer, Z. J.; Williams, K.; Manthiram, K. Understanding Continuous Lithium-Mediated Electrochemical Nitrogen Reduction. *Joule* **2019**, *3*, 1127 – 1139.

(12) Schwalbe, J. A.; Statt, M. J.; Chosy, C.; Singh, A. R.; Rohr, B. A.; Nielander, A. C.; Andersen, S. Z.; McEnaney, J. M.; Baker, J. G.; Jaramillo, T. F.; Norskov, J. K.; Cargnello, M. A Combined Theory-Experiment Analysis of the Surface Species in Lithium-Mediated NH3 Electrosynthesis. *ChemElectroChem* **2020**, *7*, 1542–1549.

(13) Skúlason, E.; Bligaard, T.; Gudmundsdóttir, S.; Studt, F.; Rossmeisl, J.; Abild-Pedersen, F.; Vegge, T.; Jónsson, H.; Nørskov, J. K. A theoretical evaluation of possible transition metal electro-catalysts for N2 reduction. *Phys. Chem. Chem. Phys.* **2012**, *14*, 1235–1245.

(14) Rostamikia, G.; Maheshwari, S.; Janik, M. J. Elementary kinetics of nitrogen electroreduction to ammonia on late transition metals. *Catal. Sci. Technol.* **2019**, *9*, 174–181.

(15) Ortuño, M. A.; Hollóczki, O.; Kirchner, B.; López, N. Selective Electrochemical Nitrogen Reduction Driven by Hydrogen Bond Interactions at Metal–Ionic Liquid Interfaces. *The Journal of Physical Chemistry Letters* **2019**, *10*, 513–517.

(16) Choi, C.; Back, S.; Kim, N.-Y.; Lim, J.; Kim, Y.-H.; Jung, Y. Suppression of Hydrogen Evolution Reaction in Electrochemical N2 Reduction Using Single-Atom Catalysts: A Computational Guideline. *ACS Catalysis* **2018**, *8*, 7517–7525.

(17) Rees, J. A.; Bjornsson, R.; Kowalska, J. K.; Lima, F. A.; Schlesier, J.; Sippel, D.; Weyhermüller, T.; Einsle, O.; Kovacs, J. A.; DeBeer, S. Comparative electronic structures of nitrogenase FeMoco and FeVco. *Dalton Trans.* **2017**, *46*, 2445–2455.

(18) Bukas, V. J.; Nørskov, J. K. A Molecular-Level Mechanism of the Biological N2 Fixation. 2019; `https://chemrxiv.org/articles/preprint/A_Molecular-Level_Mechanism_of_the_Biological_N2_Fixation/10029224/1`.

(19) Pérez-Ramírez, J.; López, N. Strategies to break linear scaling relationships. *Nature Catalysis* **2019**, *2*, 971–976.

(20) Ortuño, M. A.; Hollóczki, O.; Kirchner, B.; López, N. Selective Electrochemical Nitrogen Reduction Driven by Hydrogen Bond Interactions at Metal–Ionic Liquid Interfaces. *The Journal of Physical Chemistry Letters* **2019**, *10*, 513–517.

(21) Kibsgaard, J.; Nørskov, J. K.; Chorkendorff, I. The Difficulty of Proving Electrochemical Ammonia Synthesis. *ACS Energy Letters* **2019**, *4*, 2986–2988.

(22) Schreier, M.; Yoon, Y.; Jackson, M. N.; Surendranath, Y. Competition between H and CO for Active Sites Governs Copper-Mediated Electrosynthesis of Hydrocarbon Fuels. *Angewandte Chemie International Edition* **2018**, *57*, 10221–10225.

(23) Hu, Y.; Lee, C. C.; Ribbe, M. W. Extending the Carbon Chain: Hydrocarbon Formation Catalyzed by Vanadium/Molybdenum Nitrogenases. *Science* **2011**, *333*, 753–755.

(24) Yang, Z.-Y.; Dean, D. R.; Seefeldt, L. C. Molybdenum nitrogenase catalyzes the reduction and coupling of CO to form hydrocarbons. *The Journal of biological chemistry* **2011**, *286*, 19417–19421, 21454640[pmid].

(25) Milton, R. D.; Minteer, S. D. Nitrogenase Bioelectrochemistry for Synthesis Applications. *Accounts of Chemical Research* **2019**, *52*, 3351–3360.

(26) Singh, A. R.; Rohr, B. A.; Schwalbe, J. A.; Cargnello, M.; Chan, K.; Jaramillo, T. F.; Chorkendorff, I.; Nørskov, J. K. Electrochemical Ammonia Synthesis—The Selectivity Challenge. *ACS Catalysis* **2017**, *7*, 706–709.

(27) Bagger, A.; Ju, W.; Varela, A. S.; Strasser, P.; Rossmeisl, J. Electrochemical CO2 Reduction: A Classification Problem. *ChemPhysChem* **2017**, *18*, 3266–3273.

(28) Bagger, A.; Ju, W.; Varela, A. S.; Strasser, P.; Rossmeisl, J. Single site porphyrine-like structures advantages over metals for selective electrochemical CO2 reduction. *Catalysis Today* **2017**, *288*, 74 – 78, Electrochemical Reduction of Carbon Dioxide by heterogenous and homogeneous catalysts: Experiment and Theory.

(29) Montoya, J. H.; Tsai, C.; Vojvodic, A.; Nørskov, J. K. The Challenge of Electrochemical Ammonia Synthesis: A New Perspective on the Role of Nitrogen Scaling Relations. *ChemSusChem* **2015**, *8*, 2180–2186.

(30) Ojeda, M.; Nabar, R.; Nilekar, A. U.; Ishikawa, A.; Mavrikakis, M.; Iglesia, E. CO activation pathways and the mechanism of Fischer–Tropsch synthesis. *Journal of Catalysis* **2010**, *272*, 287 – 297.

(31) Bagger, A.; Ju, W.; Varela, A. S.; Strasser, P.; Rossmeisl, J. Electrochemical CO2 Reduction: Classifying Cu Facets. *ACS Catalysis* **2019**, *9*, 7894–7899.

(32) Sippel, D.; Rohde, M.; Netzer, J.; Trncik, C.; Gies, J.; Grunau, K.; Djurdjevic, I.; Decamps, L.; Andrade, S. L. A.; Einsle, O. A bound reaction intermediate sheds light on the mechanism of nitrogenase. *Science* **2018**, *359*, 1484–1489.

(33) Nitopi, S.; Bertheussen, E.; Scott, S. B.; Liu, X.; Engstfeld, A. K.; Horch, S.; Seger, B.; Stephens, I. E. L.; Chan, K.; Hahn, C.; Nørskov, J. K.; Jaramillo, T. F.; Chorkendorff, I. Progress and Perspectives of Electrochemical CO2 Reduction on Copper in Aqueous Electrolyte. *Chemical Reviews* **2019**, *119*, 7610–7672.

(34) Arán-Ais, R. M.; Scholten, F.; Kunze, S.; Rizo, R.; Roldan Cuenya, B. The role of in situ generated morphological motifs and Cu(i) species in C2+ product selectivity during CO2 pulsed electroreduction. *Nature Energy* **2020**, *5*, 317–325.

(35) Ju, W.; Bagger, A.; Hao, G.-P.; Varela, A. S.; Sinev, I.; Bon, V.; Roldan Cuenya, B.; Kaskel, S.; Rossmeisl, J.; Strasser, P. Understanding activity and selectivity of metal-nitrogen-doped carbon catalysts for electrochemical reduction of CO2. *Nature Communications* **2017**, *8*, 944.

(36) Boutin, E.; Wang, M.; Lin, J. C.; Mesnage, M.; Mendoza, D.; Lassalle-Kaiser, B.; Hahn, C.; Jaramillo, T. F.; Robert, M. Aqueous Electrochemical Reduction of Carbon Dioxide and Carbon Monoxide into Methanol with Cobalt Phthalocyanine.

Angewandte Chemie International Edition **2019**, *58*, 16172–16176.
(37) Spatzal, T.; Perez, K. A.; Einsle, O.; Howard, J. B.; Rees, D. C. Ligand binding to the FeMo-cofactor: Structures of CO-bound and reactivated nitrogenase. *Science* **2014**, *345*, 1620–1623.
(38) Divanis, S.; Kutlusoy, T.; Ingmer Boye, I. M.; Man, I. C.; Rossmeisl, J. Oxygen evolution reaction: a perspective on a decade of atomic scale simulations. *Chem. Sci.* **2020**, *11*, 2943–2950.
(39) Ju, W.; Bagger, A.; Wang, X.; Tsai, Y.; Luo, F.; Möller, T.; Wang, H.; Rossmeisl, J.; Varela, A. S.; Strasser, P. Unraveling Mechanistic Reaction Pathways of the Electrochemical CO2 Reduction on Fe–N–C Single-Site Catalysts. *ACS Energy Letters* **2019**, *4*, 1663–1671.
(40) Nørskov, J.; Bligaard, T.; Logadottir, A.; Bahn, S.; Hansen, L.; Bollinger, M.; Bengaard, H.; Hammer, B.; Sljivancanin, Z.; Mavrikakis, M.; Xu, Y.; Dahl, S.; Jacobsen, C. Universality in Heterogeneous Catalysis. *Journal of Catalysis* **2002**, *209*, 275–278.
(41) McEnaney, J. M.; Singh, A. R.; Schwalbe, J. A.; Kibsgaard, J.; Lin, J. C.; Cargnello, M.; Jaramillo, T. F.; Nørskov, J. K. Ammonia synthesis from N2 and H2O using a lithium cycling electrification strategy at atmospheric pressure. *Energy Environ. Sci.* **2017**, *10*, 1621–1630.
(42) Harris, D. F.; Yang, Z.-Y.; Dean, D. R.; Seefeldt, L. C.; Hoffman, B. M. Kinetic Understanding of N(2) Reduction versus H(2) Evolution at the E(4)(4H) Janus State in the Three Nitrogenases. *Biochemistry* **2018**, *57*, 5706–5714, 30183278[pmid].
(43) Sippel, D.; Rohde, M.; Netzer, J.; Trncik, C.; Gies, J.; Grunau, K.; Djurdjevic, I.; Decamps, L.; Andrade, S. L. A.; Einsle, O. A bound reaction intermediate sheds light on the mechanism of nitrogenase. *Science* **2018**, *359*, 1484–1489.
(44) Cai, R.; Minteer, S. D. Nitrogenase Bioelectrocatalysis: From Understanding Electron-Transfer Mechanisms to Energy Applications. *ACS Energy Letters* **2018**, *3*, 2736–2742.
(45) Van Stappen, C.; Decamps, L.; Cutsail, G. E.; Bjornsson, R.; Henthorn, J. T.; Birrell, J. A.; DeBeer, S. The Spectroscopy of Nitrogenases. *Chemical Reviews* **2020**, *120*, 5005–5081.
(46) Margarit, C. G.; Schnedermann, C.; Asimow, N. G.; Nocera, D. G. Carbon Dioxide Reduction by Iron Hangman Porphyrins. *Organometallics* **2019**, *38*, 1219–1223.
(47) Wan, H.; Jiao, Y.; Bagger, A.; Rossmeisl, J. Three-Dimensional Carbon Electrocatalysts for CO2 or CO Reduction. *ACS Catalysis* **2021**, *11*, 533–541.

TOC Graphic

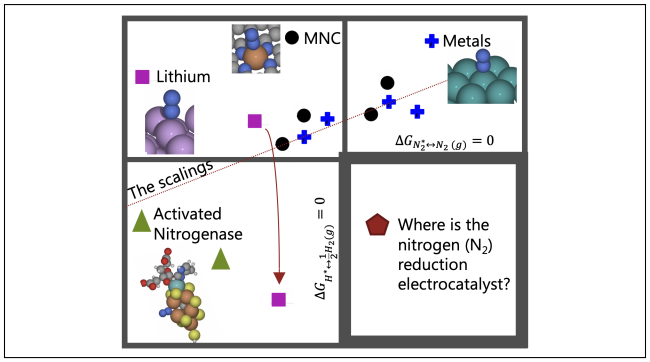
MNC
Lithium
Metals
$\Delta G_{N_2^* \leftrightarrow N_2\,(g)} = 0$
The scalings
Activated Nitrogenase
$\Delta G_{H^* \leftrightarrow \frac{1}{2}H_2(g)} = 0$
Where is the nitrogen (N_2) reduction electrocatalyst?